Journal of Renewable Materials

Tech Science Press

DOI: 10.32604/jrm.2022.018556

REVIEW

g-C_3N_4 Derived Materials for Photocatalytic Hydrogen Production: A Mini Review on Design Strategies

Kai Su[1,*], Shaoqi Deng[1], Linxiao Li[1], Qirui Qin[1], Jingyu Yang[1], Yan Chen[2,3], Shengli Zhang[1] and Junming Chen[1]

[1]Faculty of Geosciences and Environmental Engineering, Southwest Jiaotong University, Chengdu, 611756, China

[2]Analysis and Testing Center, South China Normal University, Guangzhou, 510006, China

[3]MOE Key Laboratory of Theoretical Chemistry of the Environment, School of Chemistry, South China Normal University, Guangzhou, 510006, China

[*]Corresponding Author: Kai Su. Email: ksu@swjtu.edu.cn

Received: 02 August 2021 Accepted: 20 August 2021

ABSTRACT

Hydrogen production through solar energy is one of the most important pathways to meet the growing demand of renewable energy, and photocatalyst participation in solar hydrolytic hydrogen production has received great attention in recent years in terms of low cost, high efficiency, and flexible design. Particularly, g-C_3N_4 (Graphitic-like carbon nitride material), as a unique material, can catalyze the hydrogen production process by completing the separation and transmission of charge. The easily adjustable pore structure/surface area, dimension, band-gap modulation and defect have shown great potential for hydrogen production from water cracking. In this review, the most recent advance of g-C_3N_4 including the doping of metal and non-metal elements, and the formation of semiconductor heterojunction is highlighted. The main modification strategies and approaches for the design of g-C_3N_4 for hydrogen production, as well as the influence of various materials on hydrogen evolution regarding the photocatalysis mechanism and advantages brought by theoretical calculations are specially and briefly illustrated. Potential design pathways and strategies of g-C_3N_4 are discussed. In addition, current challenges of hydrogen production from g-C_3N_4 water splitting are summarized and can be expected.

KEYWORDS

g-C_3N_4; hydrogen; photocatalysis; H_2O; semiconductor

1 Introduction

The rapid economic growth has encouraged researchers to find new forms of energy, along with the global goals for low/zero carbon dioxide emissions. The adoption of renewable energy is one of the most important pathways [1]. As renewable energy, hydrogen energy has high calorific value and clean properties [2]. Massive studies have adopted photocatalytic process to decompose pure water or waste water to relieve environmental pollutants and to obtain hydrogen energy, simultaneously [3,4]. Among the numerous materials, inorganic semiconductor materials are of low cost compared with rare metal catalysts [5]. The g-C_3N_4 polymer can induce visible light and its unique electronic structure and adaptive

capacity to adjust the band structure has attracted wide interest [6,7]. Moreover, the easy acquaintance from nature, no toxicity and strong stability of the C and N elements make them stand out.

In this regard, some preparation methods for g-C_3N_4, including the thermal condensation, solvothermal synthesis, microwave assisted synthesis, ionic liquids, and molten salt methods have been widely reported [8–10]. Meanwhile, the utilization of the precursor such as urea, melamine, thiourea and the preparation with other materials are crucial [11,12]. At present, the structure of the g-C_3N_4 models has been widely recognized, as shown in Fig. 1. Abundant modification pathways are taken to reduce the g-C_3N_4 interchange material used in catalytic hydrogen production defects, including metal or nonmetal doping, while the micro structure is modified to address the issues of generally low specific surface area, the raw carrier transfer, light electronic-hole, forbidden band width and other problems. In this review, relevant modifications of g-C_3N_4 were summarized, and the enhancement mechanisms in a hydrogen production scenario and future application challenges of the design strategies g-C_3N_4 materials were presented.

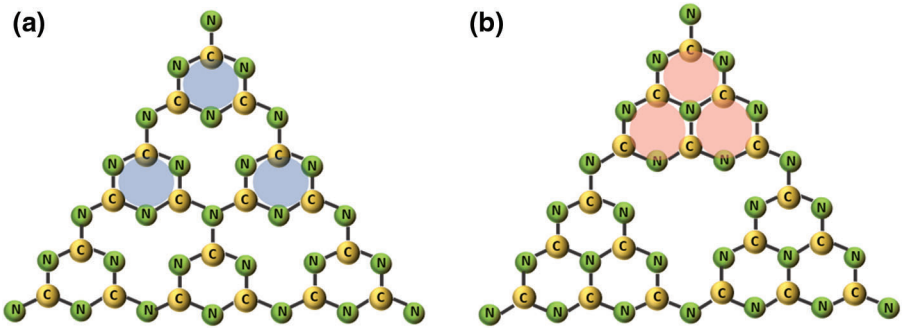

Figure 1: Structural model of g-C_3N_4: (a) S-triazine ring structure (blue shadow unit); (b) 3-s-triazine ring structure (red shadow unit)

2 Mechanism of g-C_3N_4 Photocatalysis for Hydrogen Production

As one of the most important application scenarios of g-C_3N_4 photocatalysis, hydrogen production has received a lot of attention. Based on the Gibbs free energy change ($H_2O \rightarrow H_2 + 1/2O_2$, $\Delta G = 238$ kj/mol) and thermodynamics, the splitting should meet the energy source [12]. Therefore, extra photon energy is needed to break an energy barrier of 1.23 eV. Thus, the band-energy gap of the g-C_3N_4 or the derivatives should be in the range of 1.23–3.0 eV to maintain effective splitting of water [13]. Valence band (VB) and empty conduction band (CB) can be separated by forming finite band energy gap [14]. When irradiation of incidence light is developed during the generation of photo-excited charge carrier, the exciting electrons from VB to CB can separate the e^- and h^+ pair involved in reduction and oxidation [15]. In this regard, the photocatalytic process generally includes several processes [16] (Fig. 2): (a) photon absorption; (b) exciton separation; (c) carrier diffusion, in which the low charge recombination rate decreases the charge separation rate and leads to a poor transmittance; (d) carrier transport; (e) catalysis efficiency, which decides the apparent quantum efficiency; (f) the light-generated e^-/h^+ pairs are adsorbed, followed by the movement of e^- to CB with the holes in VB, which enhances the h^+ and e^-. Through these steps, appropriate modification strategy to enhance the overall water splitting efficiency can be predicted.

There have been extensive studies on the mechanism of photocatalysis. g-C_3N_4 is very active under visible light due to the wide band gap. Considering the wide band gap of g-C_3N_4 and over-potentials, the band-energy gap ranges from 2.0 eV to 3.1 eV is higher than that of the endothermic driving forces which is about 1.23 eV but lower than visible light absorption scope [17]. The CB is higher than the potentials of H_2 production in the negative position. It is known that the sp^2 hybridization in 2D can form layered construction due to the poor van-der Waal's forces between C and N in g-C_3N_4, and the thermal

conversion process can help the condensation of feedstock with a molar ratio of 0.75 [18]. The photo-generated holes of g-C_3N_4 facilitate oxygen generation from H_2O oxidation and avert the CO_2 mineralization by strong •OH. But the low efficiency aroused by high e^-/h^+ recombination rate of smooth g-C_3N_4 has been noticed and a lot of downstream technologies focus on the enhancement of active sites, grain boundary defects and kinematics [16,17]. Additionally, researchers have widely followed the first principle based on density functional theory in the field of photocatalysis as a clear research method for effective and quick exploration to improve the g-C_3N_4 photocatalytic performance [19,20]. With the incomparable advantage of semi-empirical method like Grimme, first principle based on density functional theory has become an important basis for calculation and simulation [21]. Thus, the lattice constant, density, cell volume, relative energy, electron structure, and absorption spectra based on g-C_3N_4 can be obtained. With the calculation of band structure, density of states, and etc., it will provide more theoretical guidance for the properties and modification of g-C_3N_4. As described above, typical normal potentials of redox reaction with g-C_3N_4 band-energy gap under pH of 7 are presented in Fig. 3 [22].

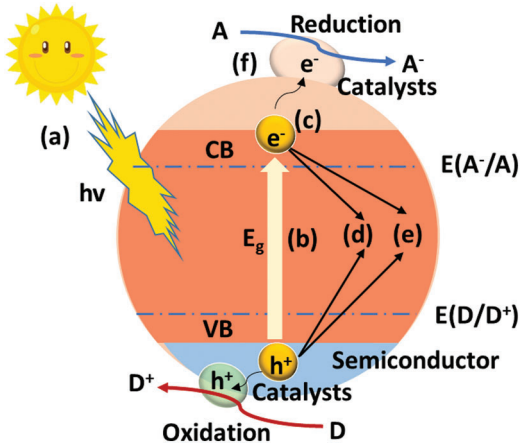

Figure 2: Mechanism of photocatalytic reaction for g-C_3N_4

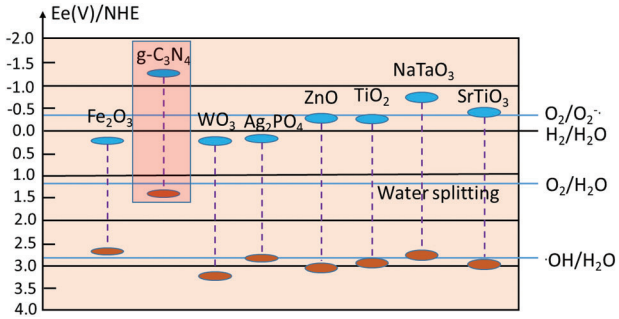

Figure 3: Typical band structures of various type of semiconductor photocatalysts compared with g-C_3N_4

3 Modification Pathways for g-C_3N_4

To modify the energy band structure of g-C_3N_4, doping metallic or nonmetallic elements by physical or chemical pathways has been proved to be effective. The light absorption, charge density, charge dispersion and mobility, as well as the crystallinity can be changed by introducing external doping elements into the semiconductor lattice. Generally speaking, nonmetals doping is realized by embedding in the body

structure of g-C_3N_4, including B, O, S, P, Cl, Br, I, and F [23–25]. It is critical to determine the location and defects of the introduced element in the skeleton structure of g-C_3N_4. For example, P element can exist in the structure matrix of g-C_3N_4 in the form of P-N bond, which makes the band gap narrow and promotes exciton separation, and some studies have found that P doping delayed the rapid recombination of electron hole pairs [25]. As for B and N, the introduction defects can broaden the visible light absorption range of g-C_3N_4, and abundant unsaturated sites can enhance the interaction of the interlayer C-N, and further promote the separation of excitons and charge transmission [26].

Generally, Mn, Zn, Cu, Ni, Fe, Co etc. are the main metal doping elements in present works [27]. Since g-C_3N_4 is a hepazine ring composed of three triazine rings along with a cavity structure formed by six unsaturated N-coordination structures, it is easy to facilitate metal elements to form metal coordination electronic structure. For example, Mn can be embedded in g-C_3N_4 as Mn-N-C group, which can adjust the positron and energy band structure, and further promote the charge transfer [27]. On this basis, researchers also try to study the influence of metal doping on g-C_3N_4 in order to optimize the strength of the metal-C-N bond or to adjust the spin state of metal ions. However, the amount of element doping is also a crucial factor. For instance, Fe doped g-C_3N_4 nanosheet structure will be cracked beyond certain Fe mass ratio. Until now, various characterization techniques including nuclear magnetic resonance, XPS, FTIR, NMR, XANES, etc., have showed that the doping elements were not only related to the size of the atomic radius of the element, but also related to the pathways and forms of the embedding. The typical doping sites of nonmatals and metals in g-C_3N_4 are shown in Figs. 4 and 5. In addition to element doping, modification of the morphology of g-C_3N_4 is another strategy, which can also modify the electronic structure, optical properties, and desirable surface characteristics. Different dimensions of g-C_3N_4 structures like carbon dots, nanorods/wires/bands/tubes/sheets/spheres/gels, etc., are defined as 0D-3D materials and show obvious differences in preparation conditions, specific surface area, exposure degree of active site, and lifetime of photogenerated carriers [28,29]. With this, secondary modification of materials with different dimensions of g-C_3N_4 and doping elements will have great potential. Nevertheless, the preparation of materials cannot be perfect due to the absence of N, C and cyanogroup, which is also called defect engineering, but this will provide opportunities for the improvement of optical properties of g-C_3N_4 [30,31].

Additionally, after the light excitation process, the electron-hole pair has a high repetition rate, which can affect the photocatalytic performance of the material. Numerous studies have proved that the formation of heterojunction structure with composite of semiconductor materials such as TiO_2, ZnO, NiS, Ni_2P, etc., and even metal organic framework (MOF) was an effective strategy to improve the photocatalytic performance of bulk g-C_3N_4 [32,33]. The heterojunction structure can be formed by seamless combination of g-C_3N_4 with carbon materials through π conjugated bonds [33]. Through the formation of heterojunction, the surface or cross linked to the crystal lattice interface inside the semiconductor can be tightly bonded and can induce the formation of internal electric field. The typical heterojunction of Type II and Z-scheme charge transfer for g-C_3N_4 are shown in Fig. 6 [34]. Specifically, the electrons in the excited state can be firstly transferred to the conduction band under the light condition, and the semiconductor with more negative conduction band position then moves forward as more positive semiconductor, while the photogenerated hole is on the opposite and accelerates the effective separation of the photogenerated electron hole pair, which is very favorable in the field of photocatalytic hydrogen production [35,36]. In a nutshell, the purpose of modification of g-C_3N_4 materials is to enhance the utilization of light and to increase the active sites and reduce the recombination of photogenerated electron-hole pairs, which will be the basis for further breakthroughs in g-C_3N_4 material innovation in the future.

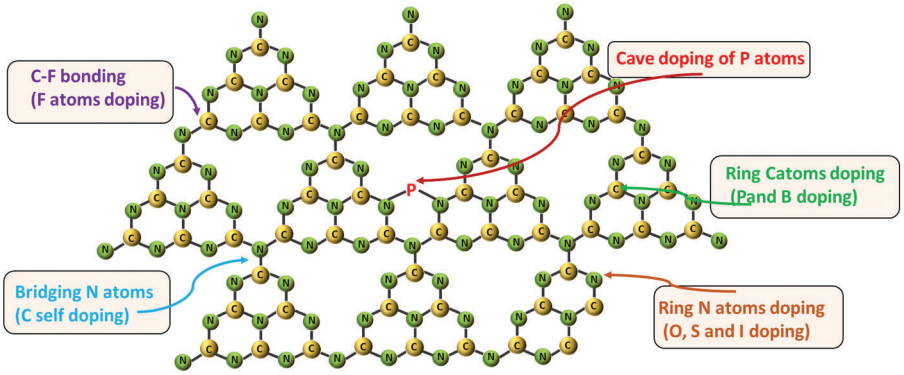

Figure 4: Potentials substituted sites of non-metals doping in a single g-C_3N_4 layer

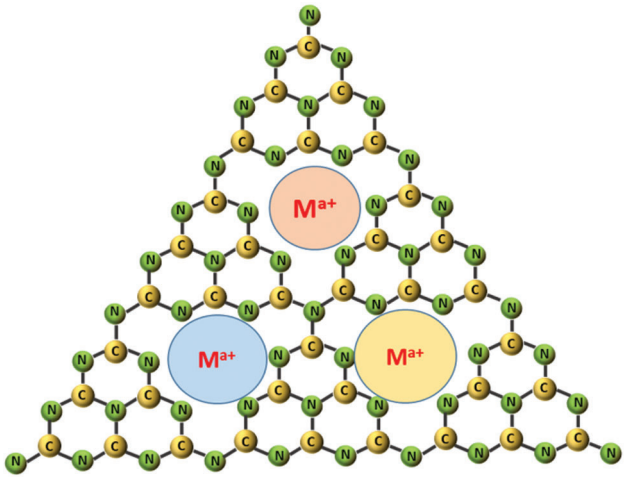

Figure 5: Typical diagram of metal ion (M^{a+}) incorporation in g-C_3N_4 framework

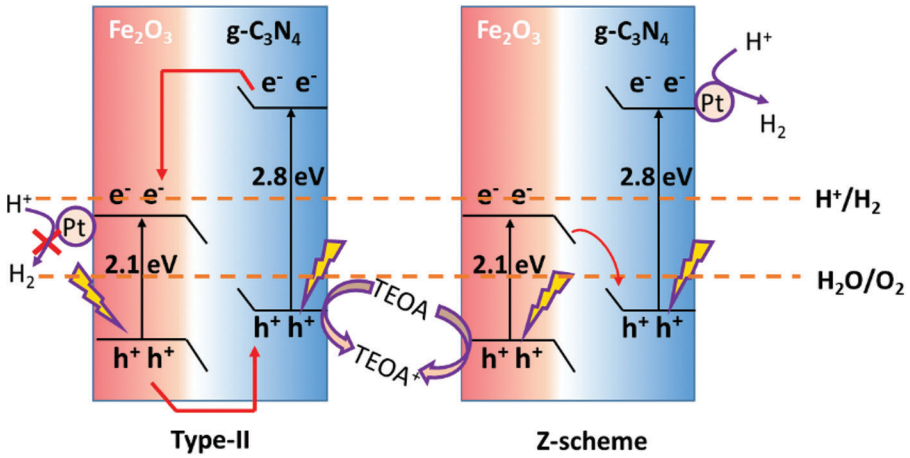

Figure 6: Typical heterojunction of Type II and Z-scheme charge transfer for g-C_3N_4

4 Design Strategies of g-C_3N_4 for H_2 Generation

The significant progress of g-C_3N_4 nanostructures tailoring techniques for catalytic H_2 generation has got a great deal of attention during the past ten years. In this section, the myriads of applications for H_2 production via water splitting were reviewed with various design strategies of g-C_3N_4 materials. For solo inorganic element doped g-C_3N_4, the H_2 generation rate can be increased by 10–20 times and more. For instance, the H_2 generation rate derived from sulfur-doped polymeric g-C_3N_4 photocatalysts reached 12.16 μmol h^{-1} [36], while the value was 57 μmol h^{-1} for P-doped g-C_3N_4 tubes [37], and 70.05 μmol h^{-1} for B doped g-C_3N_4 quantum dots [26], respectively. A lot of studies have also proved that g-C_3N_4 simultaneously doped with various species of inorganic elements or metals could also ameliorate visible-light photocatalytic H_2 generation [38,39]. For example, in Yang et al. [24]'s study, a higher surface area with optimized sp^2 conjugated heterocyclic structure was obtained for g-C_3N_4 prepared with C-I, and the hydrogen evolution rate reached 168.2 μmol/h. Generally, researchers prepared catalyst by using porous g-C_3N_4 to further modify and obtain higher efficiency of hydrogen production. Wu et al. [40] fabricated porous g-C_3N_4 nanobelts by using method of C, O binary-doped hierarchical, and the replacement of N atoms narrowed the bandgap and favored the harvest of visible-light for high H_2 evolution. In Deng et al. [41]'s work, the low electron-hole recombination rate and rapid electron transfer were found to account for the high hydrogen evolution reaction of Ni/porous g-C_3N_4. Unlike that, several works found that heterostructure could be fabricated by formation of crystal. For example, Jia et al. [42] found that $FeSe_2$/g-C_3N_4 formed nanosheets and accelerated the decomposition of H_2O_2 generation on the nanosheet surface via a stepwise two-electron/two-step pathway. In conclusion, a number of enhanced hydrogen production pathways have been demonstrated by developing and designing a robust photocatalyst. Representative g-C_3N_4 material preparation and the superiority for H_2 generation rate are summarized in Tab. 1. Meanwhile, based on the section discussed above, the design strategies of g-C_3N_4 for H_2 generation are summarized in Fig. 7.

Table 1: Representative g-C_3N_4 materials preparation and the superiority for H_2 generation rate

Precursors	Synthesis methodologies	H_2 generation rate	Superiority	References
Urea; molybdenum	Pyrolysis	327.5 μmol·g^{-1}·h^{-1}	Increased light absorption, separation and transfer of photogenerated carriers	[43]
Urea; $Ni(NO_3)_2$ and Na_2S	550°C for 4 h	992 μmol g^{-1} h^{-1}	Improved visible light absorption, promoted charge separation	[44]
urea and NH_4Cl	550°C for 3 h	-	Extend the π-conjugation; reduce the band gap and facilitate the separation of photogenerated charges	[45]
Dicyandiamide; Nickel ammonium sulfate, H_2S	600°C for 270 min	3628 μmol g^{-1} h^{-1}	Chemical bonding of Ni-S favored charge-separation	[46]
Melamine; silver nitrate	650°C for 3 h	9.728 mmol·g^{-1}·h^{-1}	Co-decoration of Ag and NiS; improved light harvesting capacity, photogenerated charge carrier separation	[47]
Melamine; Ni-MOF	550°C for 2 h	14.49 mmol g^{-1} h^{-1}	Increased the electron transfer rate staggered band alignment	[48]
Urea; graphdiyne	550°C for 2 h	39.6 μmol h^{-1}	Prolonged photogenerated charge carrier lifetime, intensified electron density, decreased reaction overpotential and improved charge carrier mobility	[49]
Melamine;	550°C for 4 h	941.80 μmol g^{-1} h^{-1}	Enhanced light absorption and high-efficiency transfer and separation of photogenerated electron hole pairs	[50]

(Continued)

Table 1 (continued)

Precursors	Synthesis methodologies	H_2 generation rate	Superiority	References
Melamine; TiO_2	300°C–700°C for 2 h	52.71 μmol h^{-1}	Wide optical absorption, separation and transportation of electronic-holes, and morphology of composite	[51]
Melamine; N-ZnO	550°C for 5 h	152.7 μmol h^{-1}	Promoted the spatial charge separation	[52]
Urea; CoS_2	550°C for 4 h	11.55 μmol h^{-1}	Improved the visible-light absorption ability and generation of photo-generated carriers	[53]
Melamine; Co doped Mo-Mo_2C	520°C for 2 h	11291 μmol h^{-1} g^{-1}	Improved interfacial charge transfer rate with low photo-generated charge recombination	[54]

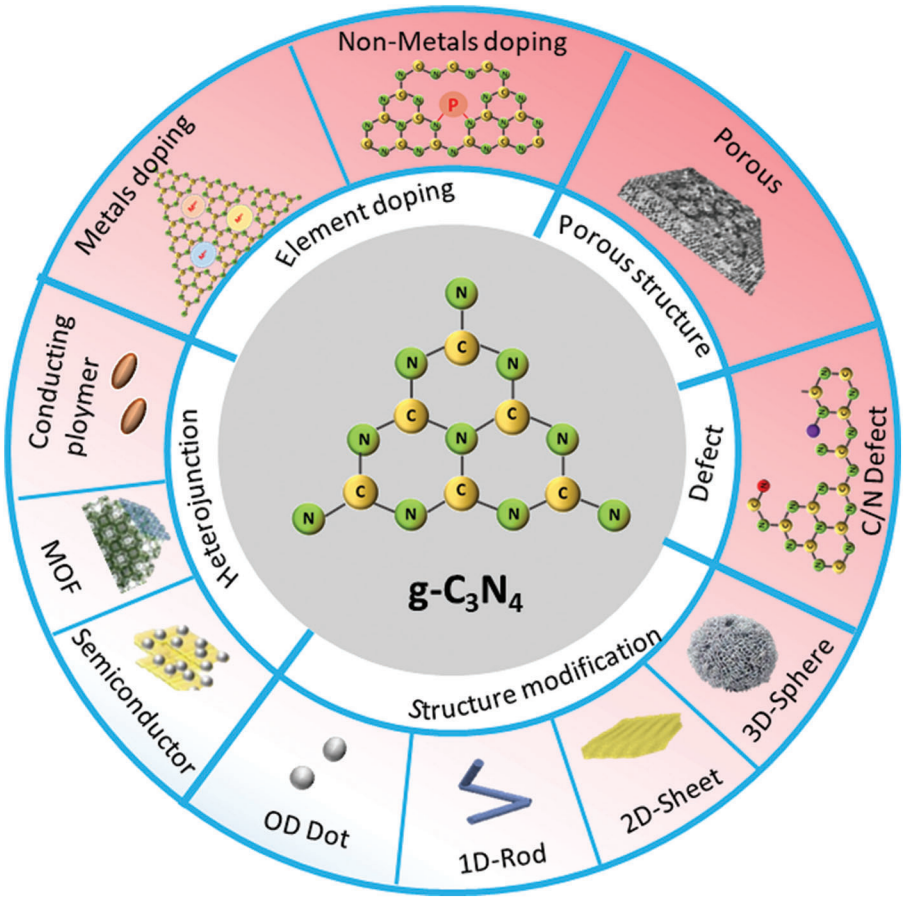

Figure 7: Design pathways and strategies of g-C_3N_4 for H_2 generation

5 Conclusion and Future Challenges

In this review, the modification pathways of g-C_3N_4 related to the elemental doping, heterojunction development and other methods were elaborated. The enhancement mechanisms in a hydrogen production scenario and future application challenges of the design strategies g-C_3N_4 materials are presented. Despite that the g-C_3N_4 materials used for photocatalytic hydrogen production have been investigated by numerous scientific works for water splitting application, the preparation, optimization of

raw materials, and the cost of hydrogen production, as well as related mechanisms of research require further extensive exploration. The detailed future challenges to overcome are as below:

(1) The durability and stability of g-C_3N_4 should be taken into more consideration regarding the recycling and efficiency.
(2) The choice of precursor feedstock for g-C_3N_4 is critical. It is essential to understand the thermal method and all other methods that can provide a better strategy for the g-C_3N_4 preparation.
(3) More morphological research should be conducted on the new heterojunction and homojunction with surface or interface characteristics and narrow absorption range.
(4) Carbonaceous semiconductors should be investigated on the metal and non-metal doping, defects, and interaction mechanisms of multiple functions, and can provide references of optimized hydrogen production rate and lower catalyst cost in the future.

Funding Statement: This work was supported by Sichuan Science and Technology Program (2021YFS0284, 2018SZDZX0026, 2021YFS0289), the Opening Project of Key Laboratory of Theoretical Chemistry of Environment (South China Normal University), Ministry of Education (20200103), the Fundamental Research Funds for the Central Universities of Southwest Jiaotong University (210824), and the Opening Project of Key Laboratory of Southwest Jiaotong University (ZD2021210001).

Conflicts of Interest: The authors declare that they have no conflicts of interest to report regarding the present study.

References

1. Abe, J. O., Popoola, A. P. I., Ajenifuja, E., Popoola, O. M. (2019). Hydrogen energy, economy and storage: Review and recommendation. *International Journal of Hydrogen Energy, 44(29),* 15072–15086. DOI 10.1016/j.ijhydene.2019.04.068.
2. Parra, D., Valverde, L., Pino, F. J., Patel, M. K. (2019). A review on the role, cost and value of hydrogen energy systems for deep decarbonisation. *Renewable & Sustainable Energy Reviews, 101,* 279–294. DOI 10.1016/j.rser.2018.11.010.
3. Qi, J., Zhang, W., Cao, R. (2018). Solar-to-hydrogen energy conversion based on water splitting. *Advanced Energy Materials, 8(5),* 1–1. DOI 10.1002/aenm.201701620.
4. Liu, W., Lu, L., Li, Q., Wu, B., Zhang, R. et al. (2020). An efficient and stable $MoS_2/Zn_{0.5}Cd_{0.5}S$ nanocatalyst for photocatalytic hydrogen evolution. *Chemistry-A European Journal, 53(26),* 12206–12211. DOI 10.1002/chem.202000821.
5. Tournet, J., Lee, Y., Karuturi, S. K., Tan, H. H., Jagadish, C. (2020). III–V Semiconductor materials for solar hydrogen production: Status and prospects. *ACS Energy Letters, 5(2),* 611–622. DOI 10.1021/acsenergylett.9b02582.
6. Shiraishi, Y., Kanazawa, S., Sugano, Y., Tsukamoto, D., Sakamoto, H. et al. (2014). Highly selective production of hydrogen peroxide on graphitic carbon nitride (g-C_3N_4) photocatalyst activated by visible light. *ACS Catalysis, 4(3),* 774–780. DOI 10.1021/cs401208c.
7. Jafarpour, M., Feizpour, F., Rezaeifard, A., Pourmorteza, N., Breit, B. (2021). Tandem photocatalysis protocol for hydrogen generation/Olefin hydrogenation using Pd-g-C_3N_4-Imine/TiO_2 nanoparticles. *Inorganic Biochemistry, 60(13),* 9484–9495. DOI 10.1021/acs.inorgchem.1c00603.
8. Kumar, A., Sharma, G., Naushad, M., Al-Muhtaseb, A. H., García-Peñas, A. et al. (2020). Bio-inspired and biomaterials-based hybrid photocatalysts for environmental detoxification: A review. *Chemical Engineering Journal, 382*, 122937. DOI 10.1016/j.cej.2019.122937.

9. Liu, X., Ma, R., Zhuang, L., Hu, B., Chen, J. et al. (2021). Recent developments of doped g-C_3N_4 photocatalysts for the degradation of organic pollutants. *Critical Reviews in Environmental Science and Technology, 51(8),* 751–790. DOI 10.1080/10643389.2020.1734433.
10. Kumar, A., Sharma, G., Kumari, A., Guo, C., Naushad, M. et al. (2021). Construction of dual Z-scheme g-C_3N_4/$Bi_4Ti^3O_{12}$/$Bi_4O_5I_2$ heterojunction for visible and solar powered coupled photocatalytic antibiotic degradation and hydrogen production: Boosting via I^-/I_3^- and Bi^{3+}/Bi^{5+} redox mediators. *Applied Catalysis, B: Environmental, 284, 119808*. DOI 10.1016/j.apcatb.2020.119808.
11. Kumar, A., Sharma, S. K., Sharma, G., Naushad, M., Stadler, F. J. (2020). CeO_2/g-C_3N_4/V_2O_5 ternary nano heterostructures decorated with CQDs for enhanced photo-reduction capabilities under different light sources: Dual Z-scheme mechanism. *Journal of Alloys and Compounds, 838, 155692*. DOI 10.1016/j.jallcom.2020.155692.
12. Takanabe, K. (2017). Photocatalytic water splitting: Quantitative approaches toward photocatalyst by design. *ACS Catalysis, 7(11),* 8006–8022. DOI 10.1021/acscatal.7b02662.
13. Yuan, L., Han, C., Yang, M. Q., Xu, Y. J. (2016). Photocatalytic water splitting for solar hydrogen generation: Fundamentals and recent advancements. *International Reviews in Physical Chemistry, 35(1),* 1–36. DOI 10.1080/0144235X.2015.1127027.
14. Malik, R., Tomer, V. K. (2021). State-of-the-art review of morphological advancements in graphitic carbon nitride (g-CN) for sustainable hydrogen production. *Renewable & Sustainable Energy Reviews, 135, 110235*. DOI 10.1016/j.rser.2020.110235.
15. Yang, Y., Niu, S., Han, D., Liu, T., Wang, G. et al. (2017). Progress in developing metal oxide nanomaterials for photoelectrochemical water splitting. *Advanced Energy Materials, 7(19),* n/a-N.PAG. DOI 10.1002/aenm.201700555.
16. Shoji, S., Peng, X., Yamaguchi, A., Watanabe, R., Fukuhara, C. et al. (2020). Photocatalytic uphill conversion of natural gas beyond the limitation of thermal reaction systems. *Nature Catalysis, 3,* 148–153. DOI 10.1038/s41929-019-0419-z.
17. Lin, B., Yang, G., Yang, B., Zhao, Y. (2016). Construction of novel three dimensionally ordered macroporous carbon nitride for highly efficient photocatalytic activity. *Applied Catalysis B: Environmental, 198,* 276–285. DOI 10.1016/j.apcatb.2016.05.069.
18. Tomer, V. K., Thangaraj, N., Gahlot, S., Kailasam, K. (2016). Cubic mesoporous Ag@CN: A high performance humidity sensor. *Nanoscale, 8(47),* 19794–19803. DOI 10.1039/c6nr08039a.
19. Ong, W. J., Tan, L. L., Ng, Y. H., Yong, S. T., Chai, S. P. (2016). Graphitic carbon nitride (g-C_3N_4)-based photocatalysts for artificial photosynthesis and environmental remediation: Are we a step closer to achieving sustainability. *Chemistry Reviews, 116(12),* 7159–7329. DOI 10.1021/acs.chemrev.6b00075.
20. Wen, J., Xie, J., Chen, X., Li, X. (2017). A review on g-C_3N_4-based photocatalysts. *Applied Surface Science, 391,* 72–123. DOI 10.1016/j.apsusc.2016.07.030.
21. Wei, B., Wang, W., Sun, J., Mei, Q., An, Z. et al. (2020). Insight into the effect of boron doping on electronic structure, photocatalytic and adsorption performance of g-C_3N_4 by first-principles study. *Applied Surface Science, 511, 145549*. DOI 10.1016/j.apsusc.2020.145549.
22. Mun, S. J., Park, S. J. (2019). Graphitic carbon nitride materials for photocatalytic hydrogen production via water splitting: A short review. *Catalysts, 9(10),* 805. DOI 10.3390/catal9100805.
23. Liu, Q., Shen, J., Yu, X., Yang, X., Liu, W. et al. (2019). Unveiling the origin of boosted photocatalytic hydrogen evolution in simultaneously (S, P, O)-Codoped and exfoliated ultrathin g-C_3N_4 nanosheets. *Applied Catalysis B: Environmental, 248,* 84–94. DOI 10.1016/j.apcatb.2019.02.020.
24. Yang, C., Teng, W., Song, Y., Cui, Y. (2018). C-I codoped porous g-C_3N_4 for superior photocatalytic hydrogen evolution. *Cuihua Xuebao/Chinese Journal of Catalysis, 39(10),* 1615–1624. DOI 10.1016/S1872-2067(18)63131-6.
25. Wu, M., Zhang, J., He, B. B., Wang, H. W., Wang, R. et al. (2019). In-situ construction of coral-like porous P-doped g-C_3N_4 tubes with hybrid 1D/2D architecture and high efficient photocatalytic hydrogen evolution. *Applied Catalysis B: Environmental, 241,* 159–166. DOI 10.1016/j.apcatb.2018.09.037.

26. Wang, Y., Li, Y., Zhao, J., Wang, J., Li, Z. (2019). g-C_3N_4/B doped g-C_3N_4 quantum dots heterojunction photocatalysts for hydrogen evolution under visible light. *International Journal of Hydrogen Energy, 44(2),* 618–628. DOI 10.1016/j.ijhydene.2018.11.067.
27. Wang, J. C., Cui, C. X., Kong, Q. Q., Ren, C. Y., Li, Z. et al. (2018). Mn-doped g-C_3N_4 nanoribbon for efficient visible-light photocatalytic water splitting coupling with methylene blue degradation. *ACS Sustainable Chemistry & Engineering, 6(7),* 8754–8761. DOI 10.1021/acssuschemeng.8b01093.
28. Liu, H., Liang, J., Fu, S., Li, L., Cui, J. et al. (2020). N doped carbon quantum dots modified defect-rich g-C_3N_4 for enhanced photocatalytic combined pollutions degradation and hydrogen evolution. *Colloids and Surfaces A: Physicochemical and Engineering Aspects, 6(8),*10200–10210. DOI 10.1016/j.colsurfa.2020.124552.
29. Wang, Y., Zhao, S., Zhang, Y., Fang, J., Chen, W. et al. (2018). Facile synthesis of self-assembled g-C_3N_4 with abundant nitrogen defects for photocatalytic hydrogen evolution. *ACS Sustainable Chemistry & Engineering, 6(8),* 10200–10210. DOI 10.1021/acssuschemeng.8b01499.
30. Liao, Y., Wang, G., Wang, J., Wang, K., Yan, S. et al. (2021). Nitrogen vacancy induced in situ g-C_3N_4 p-n homojunction for boosting visible light-driven hydrogen evolution. *Journal of Colloid and Interface Science, 587,* 110–120. DOI 10.1016/j.jcis.2020.12.009.
31. Qu, A., Xu, X., Xie, H., Zhang, Y., Li, Y. et al. (2016). Effects of calcining temperature on photocatalysis of g-c3N4/TiO2 composites for hydrogen evolution from water. *Materials Research Bulletin, 587,* 110–120. DOI 10.1016/j.materresbull.2016.03.043.
32. Jung, H., Pham, T. T., Shin, E. W. (2019). Effect of g-C_3N_4 precursors on the morphological structures of g-C_3N_4/ZnO composite photocatalysts. *Journal of Alloys and Compounds, 788,* 1084–1092. DOI 10.1016/j.jallcom.2019.03.006.
33. Liu, Q., Chen, T., Guo, Y., Zhang, Z., Fang, X. (2016). Ultrathin g-C_3N_4 nanosheets coupled with carbon nanodots as 2D/0D composites for efficient photocatalytic H_2 evolution. *Applied Catalysis B: Environmental, 193,* 248–258. DOI 10.1016/j.apcatb.2016.04.034.
34. Xu, Q., Zhu, B., Jiang, C., Cheng, B., Yu, J. (2018). Constructing 2D/2D Fe_2O_3/g-C_3N_4 direct Z-scheme photocatalysts with enhanced H_2 generation performance. *Solar RRL, 2(3),* 1800006. DOI 10.1002/solr.201800006.
35. Khan, I., Baig, N., Qurashi, A. (2019). Graphitic carbon nitride impregnated niobium oxide (g-C_3N_4/Nb2O5) type (II) heterojunctions and its synergetic solar-driven hydrogen generation. *ACS Applied Energy Materials, 2(1),* 607–615. DOI 10.1021/acsaem.8b01633.
36. Ge, L., Han, C., Xiao, X., Guo, L., Li, Y. (2013). Enhanced visible light photocatalytic hydrogen evolution of sulfur-doped polymeric g-C_3N_4 photocatalysts. *Materials Research Bulletin, 48(10),* 3919–3925. DOI 10.1016/j.materresbull.2013.06.002.
37. Guo, S., Tang, Y., Xie, Y., Tian, C., Feng, Q. et al. (2017). P-doped tubular g-C_3N_4 with surface carbon defects: Universal synthesis and enhanced visible-light photocatalytic hydrogen production. *Applied Catalysis B: Environmental, 218,* 664–671. DOI 10.1016/j.apcatb.2017.07.022.
38. Wang, M., Li, Z., Tian, L., Xie, Y., Han, J. et al. (2019). A facile synthesis of nano-layer structured g-C_3N_4 with efficient organic degradation and hydrogen evolution using a MDN energetic material as the starting precursor. *International Journal of Hydrogen Energy, 44(8),* 4102–4113. DOI 10.1016/j.ijhydene.2018.12.171.
39. Zeng, D., Ong, W. J., Chen, Y., Tee, S. Y., Chua, C. S. et al. (2018). Co_2P nanorods as an efficient cocatalyst decorated porous g-C_3N_4 nanosheets for photocatalytic hydrogen production under visible light irradiation. *Particle & Particle Systems Characterization, 35(1),* 1–1. DOI 10.1002/ppsc.201700251.
40. Wu, J., Li, N., Zhang, X. H., Fang, H. B., Zheng, Y. Z. et al. (2018). Heteroatoms binary-doped hierarchical porous g-C_3N_4 nanobelts for remarkably enhanced visible-light-driven hydrogen evolution. *Applied Catalysis, B: Environmental, 226,* 61–70. DOI 10.1016/j.apcatb.2017.12.045.
41. Deng, P., Hong, W., Cheng, Z., Zhang, L., Hou, Y. (2020). Facile fabrication of nickel/porous g-C_3N_4 by using carbon dot as template for enhanced photocatalytic hydrogen production. *International Journal of Hydrogen Energy, 45(58),* 33543–33551.DOI 10.1016/j.ijhydene.2020.09.115.

42. Jia, J., Sun, W., Zhang, Q., Zhang, X., Hu, X. et al. (2019). Inter-plane heterojunctions within 2D/2D $FeSe_2$/g-C_3N_4 nanosheet semiconductors for photocatalytic hydrogen generation. *Applied Catalysis B: Environmental, 261,* 118249. DOI 10.1016/j.apcatb.2019.118249.
43. Liu, W., Shen, J., Liu, Q., Yang, X., Tang, H. (2018). Porous MoP network structure as co-catalyst for H_2 evolution over g-C_3N_4 nanosheets. *Applied Surface Science, 462,* 822–830. DOI 10.1016/j.apsusc.2018.08.189.
44. Wen, J., Li, X., Li, H., Ma, S., He, K. et al. (2015). Enhanced visible-light H_2 evolution of g-C_3N_4 photocatalysts via the synergetic effect of amorphous NiS and cheap metal-free carbon black nanoparticles as co-catalysts. *Applied Surface Science, 358,* 204–212. DOI 10.1016/j.apsusc.2015.08.244.
45. Chuang, P. K., Wu, K. H., Yeh, T. F., Teng, H. (2016). Extending the π-conjugation of g-C_3N_4 by incorporating aromatic carbon for photocatalytic H_2 evolution from aqueous solution. *ACS Sustainable Chemistry & Engineering, 358,* 204–212. DOI 10.1021/acssuschemeng.6b01266.
46. Vu, M. H., Sakar, M., Nguyen, C. C., Do, T. O. (2018). Chemically bonded Ni cocatalyst onto the S doped g-C_3N_4 nanosheets and their synergistic enhancement in H_2 production under sunlight irradiation. *ACS Sustainable Chemistry & Engineering, 6(3),* 4194–4203. DOI 10.1021/acssuschemeng.7b04598.
47. Li, Z., Ma, Y., Hu, X., Liu, E., Fan, J. (2019). Enhanced photocatalytic H_2 production over dual-cocatalyst-modified g-C_3N_4 heterojunctions. *Cuihua Xuebao/Chinese Journal of Catalysis, 40(3),* 434–445. DOI 10.1016/S1872-2067(18)63189-4.
48. Qi, Y., Xu, J., Zhang, M., Lin, H., Wang, L. (2019). *In situ* metal–organic framework-derived c-doped Ni_3S_4/Ni_2P hybrid co-catalysts for photocatalytic H_2 production over g-C_3N_4 via dye sensitization. *International Journal of Hydrogen Energy, 44(31),* 16336–16347. DOI 10.1016/j.ijhydene.2019.04.276.
49. Xu, Q., Zhu, B., Cheng, B., Yu, J., Zhou, M. et al. (2019). Photocatalytic H_2 evolution on graphdiyne/g-C_3N_4 hybrid nanocomposites. *Applied Catalysis B: Environmental, 255,* 117770. DOI 10.1016/j.apcatb.2019.117770.
50. Feng, J., Zhang, D., Zhou, H., Pi, M., Wang, X. et al. (2018). Coupling P nanostructures with P-doped g-C_3N_4 as efficient visible light photocatalysts for H_2 evolution and RhB degradation. *ACS Sustainable Chemistry & Engineering, 6(5),* 6342–6349. DOI 10.1021/acssuschemeng.8b00140.
51. Wang, J., Huang, J., Xie, H., Qu, A. (2014). Synthesis of g-C_3N_4/TiO_2 with enhanced photocatalytic activity for H_2 evolution by a simple method. *International Journal of Hydrogen Energy, 39(12),* 6354–6363. DOI 10.1016/j.ijhydene.2014.02.020.
52. Liu, Y., Liu, H., Zhou, H., Li, T., Zhang, L. (2019). A Z-scheme mechanism of N-ZnO/g-C_3N_4 for enhanced H_2 evolution and photocatalytic degradation. *Applied Surface Science, 466,* 133–140. DOI 10.1016/j.apsusc.2018.10.027.
53. Zhang, Y., Shi, J., Huang, Z., Guan, X., Zong, S. et al. (2020). Synchronous construction of CoS_2 in-situ loading and S doping for g-C_3N_4: Enhanced photocatalytic H_2-evolution activity and mechanism insight. *Chemical Engineering Journal, 401,* 126135. DOI 10.1016/j.cej.2020.126135.
54. Zheng, Y., Dong, J., Huang, C., Xia, L., Wu, Q. et al. (2020). Co-doped Mo-Mo_2C cocatalyst for enhanced g-C_3N_4 photocatalytic H_2 evolution. *Applied Catalysis B: Environmental, 260,* 118220. DOI 10.1016/j.apcatb.2019.118220.